18. See the supplementary materials for details of the observations obtained and data reduction.
19. J. D. T. Smith *et al.*, *Astrophys. J.* **693**, 713–721 (2009).
20. K. Isensee *et al.*, *Astrophys. J.* **725**, 2059–2070 (2010).
21. H. Li, R. McCray, R. A. Sunyaev, *Astrophys. J.* **419**, 824 (1993).
22. J. M. Blondin, K. J. Borkowski, S. P. Reynolds, *Astrophys. J.* **557**, 782–791 (2001).
23. U. Hwang, M. J. Laming, *Astrophys. J.* **597**, 362–373 (2003).
24. U. Hwang, M. J. Laming, *Astrophys. J.* **746**, 130 (2012).
25. K. Eriksen, D. Arnett, D. W. McCarthy, P. Young, *Astrophys. J.* **697**, 29–36 (2009).
26. J. C. Wheeler, D. L. Meier, J. R. Wilson, *Astrophys. J.* **568**, 807–819 (2002).
27. K. Kifonidis, T. Plewa, H.-Th. Janka, E. Müller, *Astron. Astrophys.* **408**, 621–649 (2003).
28. M. Itoh, S. Kumagai, T. Shigeyama, K. Nomoto, J. Nishimura, *Nature* **330**, 233–235 (1987).
29. N. J. Hammer, H.-Th. Janka, E. Müller, *Astrophys. J.* **714**, 1371–1385 (2010).
30. W. Arnett, C. Meakin, *Astrophys. J.* **741**, 33 (2011).
31. R. A. Fesen *et al.*, *Astrophys. J.* **645**, 283–292 (2006).
32. A. Burrows, in *1604–2004: Supernovae as Cosmological Lighthouses, ASP Conference Series*, vol. 342, M. Turatto, S. Benetti, L. Zampieri, W. Shea, Eds. (Astronomical Society of the Pacific, San Francisco, CA, 2005).
33. D. Milisavljevic *et al.*, *Astrophys. J.* **751**, 25 (2012).
34. K. A. Eriksen, J. A. Morse, R. P. Kirshner, P. R. Winkler, *AIP Conf. Proc.* **565**, 193–196 (2001).

ACKNOWLEDGMENTS

This material is based on work supported by the National Science Foundation under grant no. AST-0908237, as well as observations made with the NASA/European Space Agency HST associated with Guest Observer program 10286 (Principal Investigator, R. Fesen) and obtained from the data archive at the Space Telescope Science Institute (STScI). STScI is operated by the Association of Universities for Research in Astronomy under NASA contract NAS 5-26555. Visual modeling of our observations was aided with the use of MeshLab (http://meshlab.sourceforge.net), a tool developed with the support of the 3D-CoForm project. We thank anonymous reviewers for providing suggestions that improved the content and presentation of the manuscript and D. Patnaude for helpful discussions.

SUPPLEMENTARY MATERIALS

www.sciencemag.org/content/347/6221/526/suppl/DC1
Materials and Methods
Fig. S1
References (*35*–*37*)
Movie S1

1 October 2014; accepted 23 December 2014
10.1126/science.1261949

REACTION DYNAMICS

Vibrational relaxation and microsolvation of DF after F-atom reactions in polar solvents

G. T. Dunning,[1] D. R. Glowacki,[1,2,3,4]* T. J. Preston,[1] S. J. Greaves,[5] G. M. Greetham,[6] I. P. Clark,[6] M. Towrie,[6] J. N. Harvey,[1] A. J. Orr-Ewing[1]*

Solvent-solute interactions influence the mechanisms of chemical reactions in solution, but the response of the solvent is often slower than the reactive event. Here, we report that exothermic reactions of fluorine (F) atoms in d_3-acetonitrile and d_2-dichloromethane involve efficient energy flow to vibrational motion of the deuterium fluoride (DF) product that competes with dissipation of the energy to the solvent bath, despite strong solvent coupling. Transient infrared absorption spectroscopy and molecular dynamics simulations show that after DF forms its first hydrogen bond on a subpicosecond time scale, DF vibrational relaxation and further solvent restructuring occur over more than 10 picoseconds. Characteristic dynamics of gas-phase F-atom reactions with hydrogen-containing molecules persist in polar organic solvents, and the spectral evolution of the DF products serves as a probe of solvent reorganization induced by a chemical reaction.

Elementary reactions of fluorine atoms are central to the development of our understanding of rates, dynamics, and mechanisms of chemical reactions (*1*, *2*). Evidence for rich and subtle dynamical behavior has come from studying hydrogen atom abstractions by F atoms from molecules such as H_2, H_2O, and CH_4 (or deuterium abstraction from their isotopologs) under isolated-collision conditions in the gas phase. In partnership with quantum-mechanical scattering calculations, sophisticated experiments have probed the transition state (TS) region directly (*3*, *4*), identified nonclassical processes that contribute to reaction (*5*–*8*), and observed breakdown of the Born-Oppenheimer approximation (*9*). Early TSs for these exothermic F-atom reactions favor highly vibrationally excited HF or DF molecules (*10*, *11*), consistent with expectations from the Polanyi rules (*12*). For reactions of F atoms with hydrocarbons, similar dynamics persist at the gas-liquid interface (*13*). Here, we extend mechanistic studies of F-atom reactions to the bulk liquid phase and report coupled DF-product and solvent dynamics on the picosecond time scale.

Bimolecular chemical reactions in solution are of considerable importance in both chemical synthesis and the biochemistry of living organisms. Under thermal conditions, these reactions typically occur on the ground-state potential energy surface (PES). The mechanisms of the reactions and the influence of the solvent can be explored using time-resolved spectroscopy and nonequilibrium molecular dynamics (MD) simulations (*14*–*18*), but examples of ultrafast studies of the dynamics of bimolecular reactions of thermalized reagents in liquids remain rare. The current study shows that exothermic F-atom reactions in CD_3CN or CD_2Cl_2 solutions, to produce DF and an organic radical [$\Delta_r H_0 \approx -150$ kJ mol^{-1} (*11*)], exhibit comparably rich dynamics to their gas-phase counterparts and examines the evolving postreaction microsolvation environment. The propensity of nascent DF to hydrogen bond promotes strong solute-solvent coupling, which might be expected to quench the state-specific dynamics. Nevertheless, we observe the formation of highly vibrationally excited DF, with subsequent rapid relaxation by energy transfer to the solvent bath. Evidence for a solvent response to the chemical reaction also emerges.

Figure 1 presents frames from an MD simulation that illustrate the early-time dynamics of reaction in d_3-acetonitrile. Despite reagents that are thermalized, the reaction results in strikingly nonthermal microscopic dynamics in the wake of transition-state passage. At the instant of reactive formation, DF molecules have multiple quanta of vibrational excitation, and the surrounding solvent molecules are not oriented to solvate the DF optimally. The solvent environment is thus intermediate between the noninteracting gas-phase limit and the strongly interacting equilibrium limit. Initial hydrogen-bond formation is the first step toward equilibrium solvation of the nascent DF and occurs within a few hundred femtoseconds. Subsequent time-dependent shifts in the DF vibrational frequency over several picoseconds signify both vibrational relaxation and restructuring of the microsolvation environment to accommodate this reaction product.

Figure 2 shows time-resolved infrared (TRIR) absorption spectra of DF after F-atom reactions in CD_3CN and CD_2Cl_2. One-photon photolysis of XeF_2 with 50-fs laser pulses centered at 267 nm promptly generated F atoms in solution (*19*), and DF products were probed using 50-fs IR laser pulses with >500 cm^{-1} bandwidth (*20*). The broad, unstructured IR bands are characteristic of DF solutes in organic solvents (*21*). However, the spectral features evolve in time, with a component that moves from lower to higher wave number within ~5 ps and a further shift of ~90 cm^{-1} from higher to lower wave number over the first 30 ps.

[1]School of Chemistry, University of Bristol, Cantock's Close, Bristol BS8 1TS, UK. [2]Department of Computer Science, Merchant Venturers Building, Woodland Road, Bristol BS8 1UB, UK. [3]Photon Ultrafast Laser Science and Engineering (PULSE) Institute and Department of Chemistry, Stanford University, Stanford, CA 94305, USA. [4]SLAC National Accelerator Laboratory, Menlo Park, CA 94025, USA. [5]School of Engineering and Physical Sciences, Heriot-Watt University, Edinburgh EH14 4AS, UK. [6]Central Laser Facility, Research Complex at Harwell, Science and Technology Facilities Council, Rutherford Appleton Laboratory, Harwell Oxford, Didcot, Oxfordshire OX11 0QX, UK.
***Corresponding author. E-mail: a.orr-ewing@bristol.ac.uk (A.J.O.-E.);**

Figure 2 also displays the time-dependent band intensities of the DF (v = 1 and 0) component absorptions obtained by decomposition of the time-dependent spectra (*20*). (Here, v denotes the vibrational quantum number of the DF.) This decomposition makes use of the displacement of the DF ($v = 2 \leftarrow v = 1$) absorption band by more than 100 cm^{-1} to the low wave-number side of the ($v = 1 \leftarrow v = 0$) fundamental band because of the large anharmonicity of the DF vibrational levels. The solid lines are the outcomes of fits to a kinetic model in which the F + CD_3CN or CD_2Cl_2 reaction produces DF in vibrational levels v = 2, 1, and 0, and vibrational relaxation occurs in single-quantum steps from $v = 2 \rightarrow 1$ and $v = 1 \rightarrow 0$. The kinetic fits are constrained by data derived from further experiments using ultraviolet/visible spectroscopy to monitor the reactive loss of the F atoms (*19*) (with time-constant τ_F = 4.0 ± 0.2 ps in CD_3CN and 4.5 ± 0.8 ps in CD_2Cl_2) and by IR-pump and IR-probe experiments that determined the DF($v = 1 \rightarrow 0$) vibrational relaxation time constant in solution ($\tau_{1\rightarrow0}$ = 3.1 ± 0.6 ps in CD_3CN, compared with 2.8 ± 0.3 ps from our MD simulation) (*20*). All quoted uncertainties herein correspond to 2 SDs.

We concentrate mostly on the outcomes of the F + CD_3CN reaction, for which both experimental studies and MD simulations were performed. From the fitted rate coefficients obtained from analysis of five independent data sets, we deduce a branching of 55% to DF(v = 2) and 44% to DF(v = 1) products with ±15% uncertainty and negligible direct production of DF(v = 0) molecules. Multistate reactive nonequilibrium atomistic MD simulations of the F + CD_3CN reaction in a periodic box of 62 fully flexible solvent molecules (*20*) predict very similar vibrational excitation of DF. Figure 3 illustrates the outcomes of the MD simulations for DF production and relaxation in the immediate wake of the reaction. The computed average energy in vibrational motion of the newly formed DF is almost 100 kJ mol^{-1} and mostly corresponds to DF(v = 2 and 3). Subpicosecond relaxation of the DF(v = 3) population is too fast to be resolved experimentally. The vibrational excitation decays through coupling to the solvent bath with two time constants that have a weighted average of 3.9 ± 0.18 ps, in good agreement with the experimentally determined rise of DF(v = 0) absorption.

The negative intensities assigned to DF(v = 1) in Fig. 2C indicate stimulated emission because of an initially greater population of DF(v = 2). This population inversion is sustained by faster $v = 1 \rightarrow v = 0$ than $v = 2 \rightarrow v = 1$ relaxation. Strong coupling of the DF vibrational motion to solvent modes facilitates rapid transfer of excess energy to the bath, and the solvent Fourier transform infrared (FTIR) spectrum (Fig. 2) can help identify candidate modes but cannot predict their quenching ability. The $v = 1 \leftarrow 0$ transition of incompletely solvated DF temporarily overlaps the CD_3CN vibrational mode at 2600 cm^{-1}, enabling efficient energy redistribution. In contrast, the solvent bands below 2330 cm^{-1} lie more than 100 cm^{-1} lower than the DF($v = 2 \leftarrow 1$) band center in the early time spectra. The dynamics of F-atom reactions in CD_2Cl_2 (Fig. 2D) are similar to those observed in CD_3CN, although $v = 2 \rightarrow 1$ relaxation is now found to be faster than $v = 1 \rightarrow 0$, as expected without resonant coupling to solvent modes. Initial relative populations of DF(v) levels are 77% in v = 2 and 22% in v = 1 (±11%).

We were unable to find a gas-phase study of the F + CD_3CN reaction with which to compare the liquid-phase DF(v) branching. The outcomes of measurements of HF from the F + CH_3CN reaction in the gas phase instead serve as a benchmark (*22*), and we deduce lower, but still substantial, vibration of the emergent products of reaction in solution despite the strongly interacting solvent. For the F + CD_2Cl_2 reaction, direct comparison with gas-phase data also indicates partial solvent quenching of the nascent DF vibrational excitation (*11*).

Vibrational frequencies are sensitive reporters of the local, dynamic environment of the molecule and provide information on vibrational cooling and solvent restructuring as the system approaches postreaction equilibrium. Immediately upon formation, DF is vibrationally excited and in an orientation that cannot participate in hydrogen bonding to the solvent (Fig. 1). Different types of nonequilibrium MD simulations help to reveal the microscopic mechanisms at play for short-time relaxation of the nascent DF to equilibrium. The full simulations mimicked the experiments, treating the abstraction and relaxation dynamics, and generated the transient DF spectra shown in Fig. 4. Subsequent simulations indicated two different contributions to DF relaxation in the immediate wake of the abstraction event, as a result of (i) energy flow from vibrationally excited DF to the solvent and (ii) changes in the DF microsolvation environment leading to hydrogen bonds. As shown in Fig. 4, these two dynamical relaxation processes have opposite effects on the transient DF spectra (*20*). Relaxation from more energetic vibrational quantum states drives a shift of the DF band to a higher wave number, as observed experimentally, because of the anharmonicity of the mode. Conversely, reorientation of the DF within its microsolvation environment to form hydrogen-bonded complexes shifts the DF band to lower wave number. The MD simulations predict that the latter effect causes a 220 cm^{-1} shift of the vibrational band center to lower wave number, with a time constant <1 ps that accords with previous studies of fast-solvation dynamics in acetonitrile (*23*). This process cannot be followed experimentally because of insufficient build-up of reaction products on this short time scale. However, the computational prediction is consistent with experimental observations of absorption bands below 2600 cm^{-1} at every time delay, shifted from the 2907 cm^{-1} fundamental band origin of isolated DF, and also with spectra of CD_3CN–DF complexes (*24*). The DF subsequently exchanges hydrogen-bonded solvent partners at intervals on the order of 10 ps.

The time-resolved IR spectra (Fig. 2) indicate that a second mechanism further contributes to the reduction in DF vibrational wave number on a ≤30-ps time scale. Fits to the experimental spectra incorporate a red shift of the DF($v = 0 \rightarrow 1$ and $1 \rightarrow 2$) absorption bands of 90 cm^{-1}, with a time constant of 9 to 11 ps (*20*). MD spectral analysis (e.g., Fig. 4, A1 to A3) reveals a spectral feature to the high wave-number side of the primary DF band center. This feature arises from DF molecules with a distribution of solvation environments that are not completely relaxed; solute-solvent hydrogen bonding is not fully established, even at longer times. In qualitative agreement with experimental observations, this peak eventually shifts to

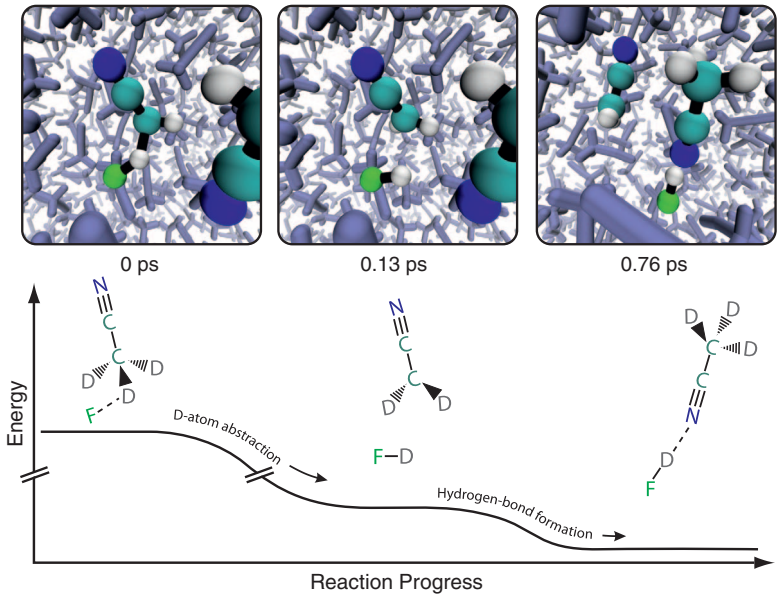

Fig. 1. Snapshots from an MD simulation of an F atom reaction in d_3-acetonitrile, superimposed on a schematic energy profile. The snapshots show the instant of transition state passage (t = 0 ps), initial separation of CD_2CN and vibrationally excited DF (t = 0.13 ps), and reorientation of the DF and a solvent molecule to establish a hydrogen bond (t = 0.76 ps). Other solvent molecules are shown in gray.

lower wave number as the DF microsolvation environment approaches equilibrium. We therefore attribute the experimentally observed spectral change to additional restructuring of the solvent around the reaction products, facilitated by hydrogen-bond dynamics (*25*). The combined experimental and computational outcomes provide the following picture for shifts in the DF fundamental frequency: The initial DF vibrational wave number approaches that of an isolated molecule [2907 cm^{-1} for DF(v = 0)], but incipient H bonding to a CD_3CN molecule with time constant <1 ps reduces it by ≥200 cm^{-1}. Further relaxation to the equilibrated 2480 cm^{-1} band center results from solvent restructuring with time constant ~10 ps. These spectral shifts oppose those associated with vibrational cooling of nascent DF(v > 0).

Multiple relaxation time scales have been observed in many solvents (*23*), and acetonitrile's extensive first- and second-solvent shell structure is consistent with their occurrence here (*26*). A similar time constant is observed for recovery of the equilibrated DF absorption spectrum when we excite a subset of the DF molecules with an IR laser tuned to be resonant only with the high wave-number wing of the fundamental band (*20*). In these latter experiments, the time constant derives solely from changes in the DF solvation environment, but for the reactive results, we cannot rule out solvent restructuring associated with replacement of XeF by one or more CD_3CN molecules after XeF_2 photolysis (*19*).

The minimum energy pathway for the reaction of an F atom with a solvent molecule in liquid CD_3CN is dominated by electronic configurations corresponding to neutral species, with negligible contributions from states deriving from D^+ transfer to the solvent [the pK_a (where K_a is the acid dissociation constant) of HF in acetonitrile is estimated to be >20 (*27*)]. However, at the energies of vibrationally excited DF, our MD simulations demonstrate the transient influence of diabatic states with deuteron-transfer character on the products' side of the TS. These states are required for an accurate description of the anharmonicity in the solute-solvent coupling and must be included in our treatment of the reaction PES to give the reported agreement between the MD simulations and experimental measurements of energy disposal to the DF and its subsequent relaxation to the solvent bath.

The current work extends to the liquid-phase prior dynamical studies of benchmark fluorine-atom reactions with organic molecules. As we have found in other bimolecular reactions (*14*, *16*), we can apply, with certain caveats, intuition derived from the gas-phase reaction dynamics to the complicated realm of liquids. Despite strong solute-solvent coupling, highly vibrationally excited DF products form after reaction in liquid CD_3CN and CD_2Cl_2, but this excitation is lower than for reactions in the gas phase. Solvent damping of the nascent DF vibration may derive from coupling

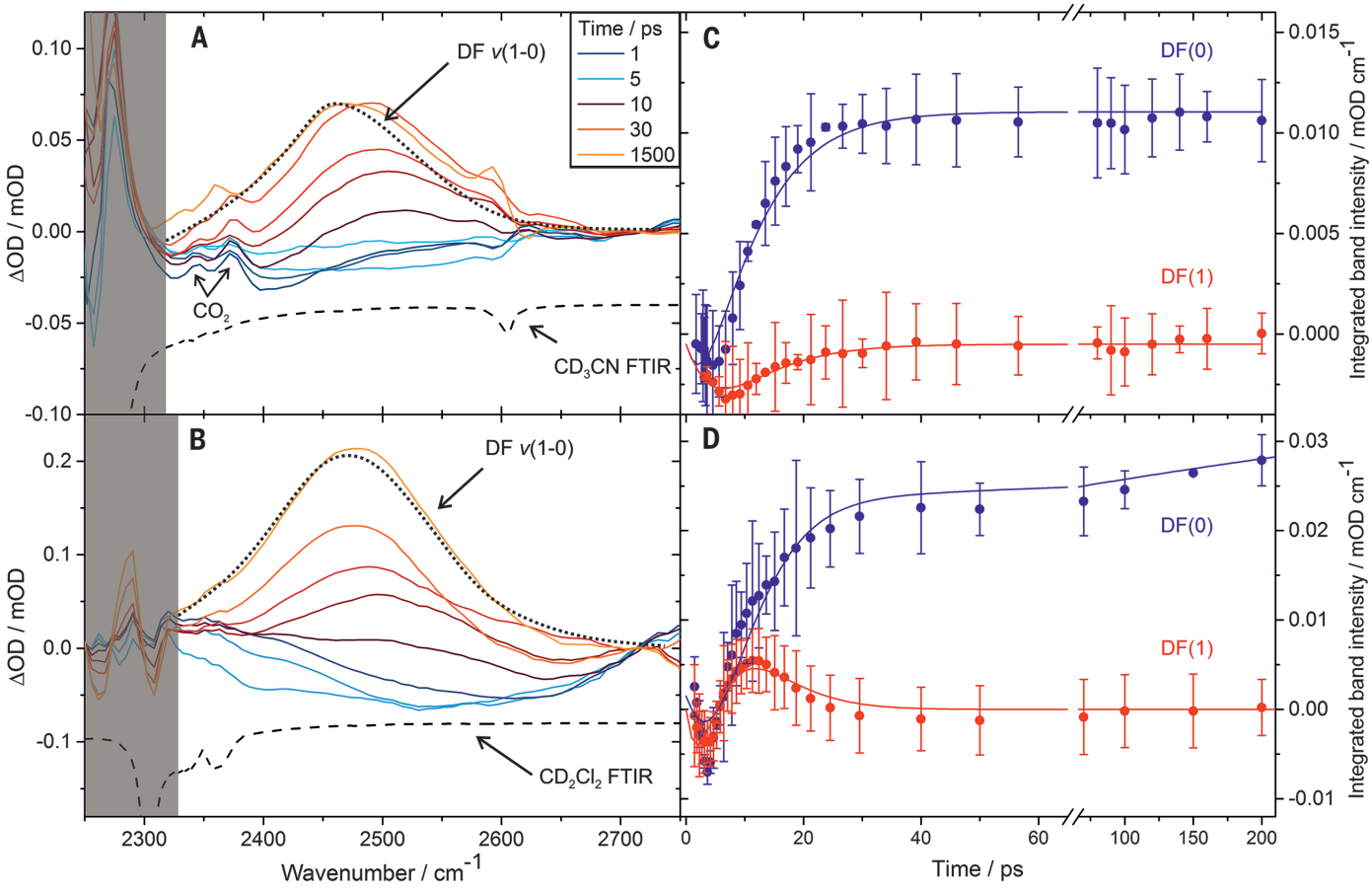

Fig. 2. TRIR absorption spectra and DF band intensities for reactions of F atoms in polar solvents. (**A** and **C**) Results in CD_3CN. (**B** and **D**) Results in CD_2Cl_2. The inset key shows selected time delays at which the transient spectra were obtained. Negative intensities indicate stimulated emission because of vibrational population inversions. The black dotted lines are steady-state FTIR spectra of DF in each solvent, and inverted solvent spectra are shown as dashed lines. Gray shading masks regions of strong solvent absorption. Decomposition of the spectra into $v = 1 \leftarrow v = 0$ and $v = 2 \leftarrow v = 1$ bands uses the anharmonicity of the DF vibrational levels, which shifts the (2 ← 1) band more than 100 cm^{-1} lower than the (1 ← 0) band. Fitting of time-resolved spectra for complete sets of time delays, subsets of which are shown in (A) and (B), gives the integrated DF(v = 0) (blue circles) and DF(v = 1) (red circles) absorption band intensities in (C) and (D), respectively. Uncertainties (2-SD error bars) are obtained from comparison of the fitted band intensities for separately acquired sets of time-resolved spectra and illustrate the reproducibility of the results. Kinetic fits (solid lines) use a model described in the supplementary materials (*20*): Independent fits to separately acquired sets of pairs of time-dependent (2 ← 1) and (1 ← 0) band intensities give the rate coefficients, mean values, and 2-SD uncertainties (from five data sets for F + CD_3CN and three for F + CD_2Cl_2) presented in tables S1 and S2.

to the energized products as they emerge from the TS and displacement of the TS later along the reaction coordinate. Equilibration of the excess DF vibrational energy takes 3 to 4 ps in both solvents. Further solvent restructuring to accommodate reaction products continues over the ensuing 10 ps. This depth of understanding of a condensed-phase reaction mechanism requires knowledge not only of the PES but also of the dynamical interplay between solute and solvent. Vibrational probes of reactions in solution and nonequilibrium MD simulations provide penetrating insights into the dynamics of bond-making and subsequent dissipation of excess chemical energy to the solvent. Further exploration using this combined methodology will provide increasingly detailed descriptions of the effect of emergent product vibrational excitation on reaction outcomes in complex systems.

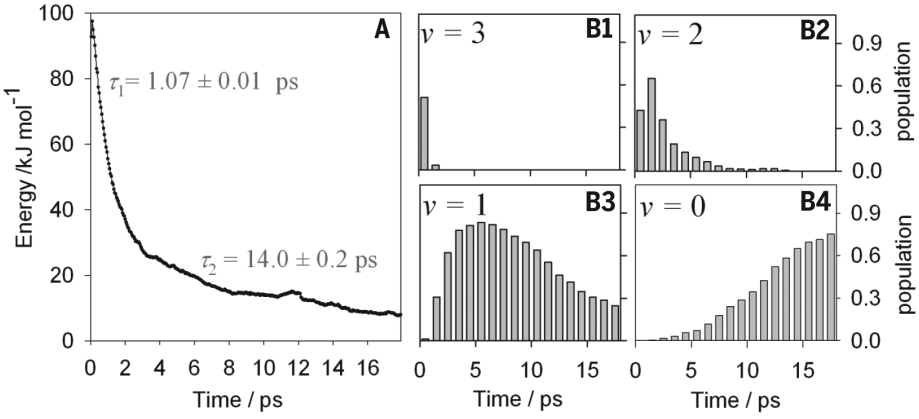

Fig. 3. Transient DF vibrational energy content following D-atom abstractions in d_3-acetonitrile, obtained from the MD simulations. (**A**) DF vibrational energy averaged over 200 trajectories, with time constants obtained from a biexponential fit. (**B1** to **B4**) Normalized transient vibrational energy content in the v = 0 to 3 vibrational levels. Exponential fits to the decaying populations of v = 3, 2, and 1 and the rise in v = 0 give time constants of $\tau_{3\to2}$ = 0.37 ± 0.20 ps, $\tau_{2\to1}$ = 3.6 ± 1.8 ps, and $\tau_{1\to0}$ = 6.9 ± 1.4 ps.

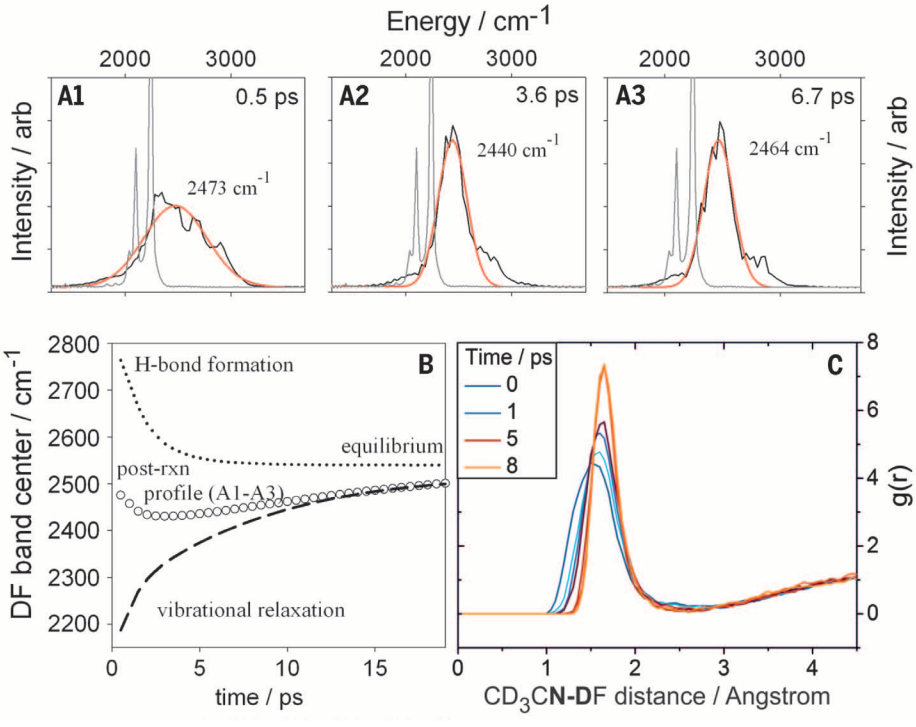

Fig. 4. MD simulations of transient power spectra and radial distribution functions. (**A**) Transient DF spectral bands (black lines), Gaussian fits to the simulated DF spectra (red lines), and the simulated solvent spectrum (gray lines). (**B**) Time-dependent postreaction profile of the DF band center (circles), together with results from separate simulations that identify spectral effects of hydrogen-bond formation with CD_3CN (dotted line) and relaxation of vibrationally excited DF (dashed line). (**C**) Time evolution of the radial distribution function, $g(r)$, which describes the changing distribution of distances of the D atom (in DF) to the N atoms of the CD_3CN solvent molecules.

REFERENCES AND NOTES

1. R. D. Levine, *Molecular Reaction Dynamics* (Cambridge Univ. Press, Cambridge, 2005).
2. D. M. Neumark, A. M. Wodtke, G. N. Robinson, C. C. Hayden, Y. T. Lee, *J. Chem. Phys.* **82**, 3045–3066 (1985).
3. W. Dong *et al.*, *Science* **327**, 1501–1502 (2010).
4. D. E. Manolopoulos *et al.*, *Science* **262**, 1852–1855 (1993).
5. M. Tizniti *et al.*, *Nat. Chem.* **6**, 141–145 (2014).
6. M. Qiu *et al.*, *Science* **311**, 1440–1443 (2006).
7. T. Wang *et al.*, *Science* **342**, 1499–1502 (2013).
8. R. Otto *et al.*, *Science* **343**, 396–399 (2014).
9. L. Che *et al.*, *Science* **317**, 1061–1064 (2007).
10. J. J. Lin, J. Zhou, W. Shiu, K. Liu, *Science* **300**, 966–969 (2003).
11. M. A. Wickramaaratchi, D. W. Setser, H. Hildebrandt, B. Körbitzer, H. Heydtmann, *Chem. Phys.* **94**, 109–129 (1985).
12. J. C. Polanyi, *Acc. Chem. Res.* **5**, 161–168 (1972).
13. A. M. Zolot, P. J. Dagdigian, D. J. Nesbitt, *J. Chem. Phys.* **129**, 194705 (2008).
14. S. J. Greaves *et al.*, *Science* **331**, 1423–1426 (2011).
15. R. A. Rose *et al.*, *J. Chem. Phys.* **134**, 244503 (2011).
16. A. J. Orr-Ewing, *J. Chem. Phys.* **140**, 090901 (2014).
17. D. R. Glowacki, A. J. Orr-Ewing, J. N. Harvey, *J. Chem. Phys.* **134**, 214508–214511 (2011).
18. D. R. Glowacki, R. A. Rose, S. J. Greaves, A. J. Orr-Ewing, J. N. Harvey, *Nat. Chem.* **3**, 850–855 (2011).
19. G. T. Dunning *et al.*, *Phys. Chem. Chem. Phys.* **16**, 16095–16102 (2014).
20. Materials and methods are available as supporting material on *Science* Online.
21. R. M. Adams, J. J. Katz, *J. Mol. Spectrosc.* **1**, 306–332 (1957).
22. K. Dehe, H. Heydtmann, *Chem. Phys. Lett.* **262**, 683–688 (1996).
23. B. Bagchi, B. Jana, *Chem. Soc. Rev.* **39**, 1936–1954 (2010).
24. G. L. Johnson, L. Andrews, *J. Phys. Chem.* **87**, 1852–1859 (1983).
25. R. Rey, K. B. Møller, J. T. Hynes, *J. Phys. Chem. A* **106**, 11993–11996 (2002).
26. W. L. Jorgensen, J. M. Briggs, *Mol. Phys.* **63**, 547–558 (1988).
27. C. R. Nicoleti, V. G. Marini, L. M. Zimmermann, V. G. Machado, *J. Braz. Chem. Soc.* **23**, 1488–1500 (2012).

ACKNOWLEDGMENTS

The Bristol group thanks the Engineering and Physical Sciences Research Council (EPSRC, Programme Grant EP/G00224X and a studentship for G.T.D.) and the European Research Council (ERC, Advanced Grant 290966 CAPRI) for financial support. D.R.G. acknowledges award of a Royal Society University Research fellowship, J.N.H. acknowledges a Royal Society Wolfson Merit Award, and S.J.G. thanks EPSRC for award of a Career Acceleration Fellowship (EPSRC EP/J002534/2). Experimental measurements were conducted at the ULTRA Laser Facility, which is supported by the Science and Technology Facilities Council (STFC, Facility Grant ST/501784). We are grateful to F. Abou-Chahine for assistance with collection of some of the experimental data and to M. P. Grubb and M. N. R. Ashfold for valuable discussions. All experimental data and analysis files are archived in the University of Bristol's Research Data Storage Facility. The supplementary materials contain summaries of the data analysis procedures and outcomes. Individual contributions to the work: A.J.O.-E. and G.T.D. devised and carried out the experiments, with assistance from S.J.G., and analyzed the experimental data with T.J.P. and S.J.G. G.M.G., I.P.C., and M.T. constructed and operated the ultrafast laser system at the Central Laser Facility, with which all experimental data were collected. D.R.G. and J.N.H. devised and performed the MD simulations and analyzed the computational results. A.J.O.-E., G.T.D., T.J.P., D.R.G., and J.N.H. wrote the paper.

SUPPLEMENTARY MATERIALS

www.sciencemag.org/content/347/6221/530/suppl/DC1
Materials and Methods
Figs. S1 to S7
Tables S1 to S2
References (*28*–*51*)

8 October 2014; accepted 29 December 2014
10.1126/science.aaa0103

Vibrational relaxation and microsolvation of DF after F-atom reactions in polar solvents

G. T. Dunning *et al.*

Science **347**, 530 (2015);
DOI: 10.1126/science.aaa0103